

## Theory of the Nonhydrogenic Stark Effect

David A. Harmin<sup>(a)</sup>*Department of Physics, University of Chicago, Chicago, Illinois 60637*

(Received 12 April 1982)

Photoionization spectra of alkali atoms in a dc electric field are calculated semianalytically and agree with experiment. Cross sections depend on two distinct sets of parameters: (a) zero-field dipole matrix elements and quantum defects and (b) eigenfunctions of the external Coulomb-Stark potential. The field's effect on photoionization is condensed into a density-of-states matrix  $\langle \Psi' | \Psi \rangle^{-1}$ , whose use may be appropriate to long-range effects in all spectral phenomena.

PACS numbers: 32.60.+i, 32.70.-n, 32.80.Fb

Observations of the dc Stark effect near threshold in alkalis led to the discovery by Freeman *et al.*<sup>1</sup> of resonances extending into the ionization continuum. Figure 1(a) shows a recent photoionization spectrum of Na  $3^2P_{3/2}$  from Luk *et al.*<sup>2</sup> The region below threshold exhibits asymmetric resonance peaks, whereas above threshold one observes only a series of modulations. I report here the result of a calculation, shown in Fig. 1(b), which reproduces the experimental data; details of the theory and of the calculation will be reported elsewhere.<sup>3</sup> The presence of a nonhydrogenic core produces the interference dips

below threshold, but only attenuates the modulations above threshold calculated for the simple case of hydrogen.<sup>4,5</sup>

The calculation uses two distinct types of input parameters: (a) *zero-field* spectral parameters of the atom, namely, dipole matrix elements and quantum defects,<sup>6</sup> and (b) semianalytical parameters of the wave function in the Coulomb + Stark potential (in atomic units),

$$V(\vec{r}) = -1/r + Fz, \quad (1)$$

which prevails outside the Na<sup>+</sup> core. These parameters are obtained with sufficient accuracy

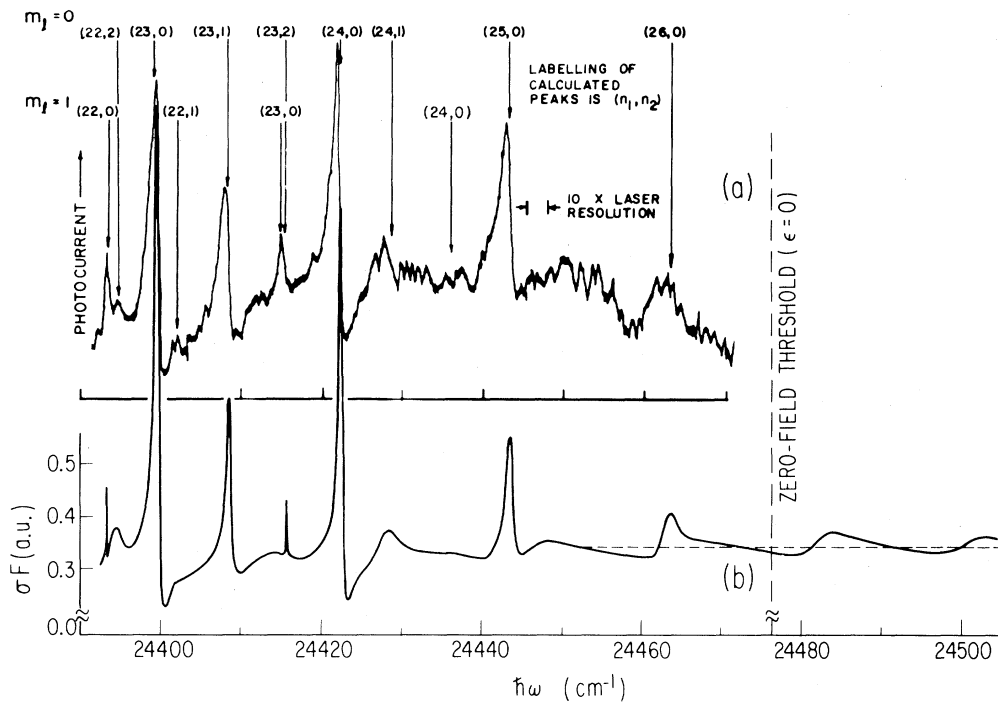


FIG. 1. (a) Experimental photoionization spectrum of Na  $3^2P_{3/2}$  in a field  $F = 3.59$  kV/cm, vs photon energy  $\hbar\omega$ , just below threshold (Ref. 2). Note labeling of Stark resonances. (b) Theoretical cross section  $\sigma^F$ , Eq. (12); dashed line,  $\sigma^{F=0}$ . Asymmetric peaks labeled as for (a). Stark-induced oscillations extend past  $\epsilon = 0$  with the same spacing as in H ( $19.6$   $\text{cm}^{-1}$ ).

by a WKB analysis of the Stark effect in H.<sup>4</sup>

The separation of these effects is made possible by the remark<sup>4,7</sup> that the Stark potential in Eq. (1) is negligible compared to the Coulomb term when  $r \ll F^{-1/2}$  a.u. (1 a.u. =  $5.14 \times 10^8$  kV/cm). Over the range of distances

$$r_0 \sim 1 \text{ a.u.} \lesssim r \ll F^{-1/2} \text{ a.u.} \quad (2)$$

the potential surrounding the Na<sup>+</sup> core is represented by just the Coulomb term of (1), and the Schrödinger equation is *equally separable* in spherical and parabolic coordinates.<sup>8</sup> The Coulomb region (2) thus marks the overlap of regions of spherical symmetry,  $r \ll F^{-1/2}$  a.u., and parabolic symmetry,  $r > r_0$ . The photoabsorption process proper is handled by standard atomic procedures in spherical coordinates, ignoring the Stark field. The subsequent escape of the electron is then treated in parabolic coordinates, appropriate to the external Coulomb-Stark potential.

The wave function of the excited electron following photoabsorption, within the radial range (2), is represented in spherical coordinates by<sup>9</sup>

$$\Psi_{lm}(\vec{r}) = \cos \delta_l f_{lm}(\vec{r}) - \sin \delta_l g_{lm}(\vec{r}), \quad (3)$$

where the quantum defects  $\mu_l = \delta_l/\pi$  are taken on the branch  $-\frac{1}{2} < \mu_l < +\frac{1}{2}$ , and the value  $\epsilon$  of the energy is omitted. The function  $f_{lm}(\vec{r})$  is a hydrogen function regular at  $r=0$ , including both the spherical harmonic  $Y_{lm}(\theta, \varphi)$  and the radial Coulomb function, while the irregular function  $g_{lm}(\vec{r})$  lags in  $r$  by  $90^\circ$  with respect to  $f_{lm}(\vec{r})$  but has the same energy-normalization amplitude at large  $r$ .

The regular and irregular parabolic functions analogous to  $f_{lm}(\vec{r})$  and  $g_{lm}(\vec{r})$  are called here  $\psi_{\beta m}^F(\vec{r})$  and  $\chi_{\beta m}^F(\vec{r})$ . Separation of variables in the parabolic coordinates<sup>10</sup>  $\{\xi = r(1 + \cos \theta), \eta = r(1 - \cos \theta), \varphi\}$  yields

$$\psi_{\beta m}^F(\vec{r}) = [e^{im\varphi} (2\pi)^{-1/2}] \Xi_{\beta m}^F(\xi) \Upsilon_{\beta m}^F(\eta), \quad (4a)$$

$$\chi_{\beta m}^F(\vec{r}) = [e^{im\varphi} (2\pi)^{-1/2}] \Xi_{\beta m}^F(\xi) \bar{\Upsilon}_{\beta m}^F(\eta). \quad (4b)$$

The azimuthal factors in (4a) and (4b) appear also in  $Y_{lm}(\theta, \varphi)$ , but  $P_{lm}(\cos \theta)$  is replaced here by an eigenfunction  $\Xi_{\beta m}^F(\xi)$  of the upfield coordinate  $\xi$ . The separation parameter  $\beta \equiv \beta(\epsilon, F; n_l,$

$m)$  is the effective charge allocated to  $\xi$  (with  $1 - \beta$  going to  $\eta$ ). The eigenvalues of  $\beta$  are set at each  $\epsilon$ ,  $F$ , and  $m$  by the number  $n_l = 0, 1, 2, \dots$  of nodes of the wave function  $\Xi_{\beta m}^F(\xi)$ , which is bound by the rise of the potential (1) as  $\xi \rightarrow \infty$ .

The regular function  $\Upsilon(\eta)$  is normalized per unit energy and oscillates at  $\eta \rightarrow \infty$  as an Airy function; for  $\epsilon < \epsilon_c = -2[(1 - \beta)F]^{1/2}$  it tunnels in  $\eta$  through a broad barrier of the potential (1). The irregular function  $\bar{\Upsilon}$  in Eq. (4b) has the same energy-normalization amplitude as  $\Upsilon$  at  $\eta \rightarrow \infty$  but its oscillations lag in phase by  $90^\circ$  in the range (2). However, the oscillations of  $\bar{\Upsilon}$  with respect to  $\Upsilon$  outside the barrier, as  $\eta \rightarrow \infty$ , lag instead by a phase parameter  $\gamma_\beta$  ( $0 < \gamma_\beta < \pi$ ), which reduces again to  $\frac{1}{2}\pi$  only at energies sufficiently above  $\epsilon_c$ .<sup>3</sup>

The connection between the spherical and parabolic basis functions (3) and (4) is established first by a transformation  $U_{\beta l}$  between the *regular* functions,

$$\begin{aligned} \psi_\beta^F(\vec{r}) &= \sum_l U_{\beta l} f_l(\vec{r}), \\ f_l(\vec{r}) &= \sum_\beta (U^{-1})_{l\beta} \psi_\beta^F(\vec{r}), \end{aligned} \quad (5)$$

where the sums extend over all  $l$  or  $\beta$  (i.e.,  $n_l$ ), and I have omitted the common subscript  $m$ . The matrix element

$$U_{\beta l} = a_{\beta l} N_\beta^F / N_l \quad (6)$$

from Ref. 7 depends explicitly on the energy-normalizing amplitudes  $N_l$  of  $f_l$  and  $N_\beta^F$  of  $\psi_\beta^F$  [called  $(N_{\epsilon n_l m}^F)^{1/2}$  in Ref. 4], whose squares represent the spectral density of states of each channel. The coordinate transformation  $a_{\beta l}$  is a polynomial of degree  $l - m$  in  $2\beta - 1$ . Note that at constant  $\epsilon$ ,  $U_{\beta l}$  is *nonorthogonal* unless  $F = 0$ , because  $f_l$  and  $\psi_\beta^F$  pertain to different potentials at  $r \rightarrow \infty$ .<sup>3</sup>

The analog of the transformation (5) for the irregular functions follows from a key remark by Fano<sup>7</sup>: The irregular component in Eq. (3) arises from the departure of the Na<sup>+</sup> core potential from a pure Coulomb potential at  $r < r_0$ . The standing-wave Green's function  $G^c(\vec{r}, \vec{r}')$  that propagates this potential inhomogeneity is a solution of the Schrödinger equation for the Coulomb potential alone, and must therefore *coincide* in spherical and parabolic coordinates:

$$G^c(\vec{r}, \vec{r}') = \pi \sum_{lm} g_l(\vec{r}) f_l(\vec{r}') = \pi \sum_{\beta m} \chi_\beta^F(\vec{r}) \text{csc} \gamma_\beta \psi_\beta^F(\vec{r}'), \quad r' < r \ll F^{-1/2}. \quad (7)$$

The important factor  $\text{csc} \gamma_\beta$  arises from the change in the relative normalizations of  $\Upsilon(\eta)$  and  $\bar{\Upsilon}(\eta)$  across the barrier of the potential (1). Equations (5) and (7) imply the transformation of the irregular

functions,

$$\chi_{\beta}^F(\vec{r}) = \sum_i \sin \gamma_{\beta} (\tilde{U}^{-1})_{\beta i} g_i(\vec{r}), \quad g_i(\vec{r}) = \sum_{\beta} \tilde{U}_{i\beta} \csc \gamma_{\beta} \chi_{\beta}^F(\vec{r}). \quad (8)$$

The continuation of the final-state function (3) beyond the region (2), i.e., to where the Stark field becomes important, is thus represented in parabolic coordinates through Eqs. (5) and (8) by

$$\Psi_i(\vec{r}) = \cos \delta_i \sum_{\beta} (U^{-1})_{i\beta} \psi_{\beta}^F(\vec{r}) - \sin \delta_i \sum_{\beta} \tilde{U}_{i\beta} \csc \gamma_{\beta} \chi_{\beta}^F(\vec{r}). \quad (9)$$

Finally, it is the superposition (9) which must be normalized per unit energy, thus combining the effects of (a) the short-range spherical phase shifts  $\delta_i$  due to the  $\text{Na}^+$  core, (b) the long-range parabolic phase shifts  $\gamma_{\beta}$  due to the Coulomb-Stark barrier, and (c) the transformation  $U_{\beta}$ , Eq. (6). Normalization utilizes the overlap matrix of the set  $\{\Psi_i\}$ ,

$$\langle \Psi_{i'} | \Psi_i \rangle = \{ (\cos \delta - \sin \delta h^F) (H^F)^{-1} (\cos \delta - h^F \sin \delta) + \sin \delta H^F \sin \delta \}_{i' i} \delta_{m' m} \delta(\epsilon' - \epsilon), \quad (10)$$

$$H^F \equiv \tilde{U} U, \quad h^F \equiv \tilde{U} \cot \gamma U, \quad (11)$$

with  $\cos \delta$ ,  $\sin \delta$ , and  $\cot \gamma$  diagonal matrices and the cross-term overlap  $\langle \chi_{\beta' m'}^F | \psi_{\beta m}^F \rangle = \cos \gamma_{\beta} \delta(\epsilon' - \epsilon) \times \delta_{\beta' \beta} \delta_{m' m}$ .

The photoabsorption cross section now reads

$$\sigma^F = \frac{4\pi^2}{137} \hbar \omega \sum_{i', i} \langle 0 | r_m | \Psi_{i'} \rangle [ \langle \Psi' | \Psi \rangle^{-1} ]_{i' i} \langle \Psi_i | r_m | 0 \rangle, \quad (12)$$

where  $|0\rangle$  is the initial state of the atom,  $r_m = z$  for  $\pi$ -polarized light, and  $r_m = (1/\sqrt{2})(x \pm iy)$  for  $\sigma^{\pm}$  polarization. Matrix inversion of (10) does not apply to  $\delta(\epsilon' - \epsilon)$ , which has been absorbed into the dipole matrix elements. Equation (12) thus sorts out (a) atomic contributions, i.e., zero-field dipole matrix elements  $\langle \Psi_i | r | 0 \rangle$  and the  $\cos \delta_i$  and  $\sin \delta_i$  terms from the overlap matrix (10), and (b) Stark effects embodied in the matrices  $H_{i' i}^F$  and  $h_{i' i}^F$ . The factor  $\langle \Psi' | \Psi \rangle^{-1}$  thus acts as a "density-of-states" matrix which modulates the distribution of zero-field oscillator strengths.<sup>11</sup> In hydrogen all  $\delta_i = 0$  and  $\langle \Psi' | \Psi \rangle^{-1}$  is just  $H^F$ . For other atoms inversion of the symmetric matrix (10) is required only in the subspace where  $\delta_i \neq 0$ .<sup>12</sup>

A typical resonance profile below threshold reduces to the form<sup>13</sup>

$$[ \langle \Psi' | \Psi \rangle^{-1} ]_{ii} = H_{ii}^F \frac{1 + \tan^2 \delta_i}{(1 - h_{ii}^F \tan \delta_i)^2 + (H_{ii}^F \tan \delta_i)^2}, \quad (13)$$

where  $H_{ii}^F$  is Lorentzian,  $h_{ii}^F$  is its dispersive companion, and both include a background from nonresonant channels. This expression is recast as a Beutler-Fano profile in Ref. 3. It is made asymmetric by the factor  $\cot \gamma$  included in  $h^F$ , whose sign reverses as  $\gamma$  increases rapidly by  $\approx \pi$  through a resonance. We see from Eqs. (12) and (13) that the interference dip will lie on the high- (low-) energy side of a resonance for  $\mu_i > 0$  ( $\mu_i < 0$ ); cf. Fig. 1(b) for Na, with  $\mu_0 = 1.35$ . Above threshold these interference effects disappear (all  $\gamma_{\beta} = \frac{1}{2}\pi$  so that  $h^F = 0$ ) and Eq. (13) is approximately

$$[ \langle \Psi' | \Psi \rangle^{-1} ]_{ii} = 1 + (H_{ii}^F - 1) \cos 2\pi \mu_i, \quad \epsilon \gtrsim 0, \quad (14)$$

assuming  $H_{ii}^F - 1 = O(10^{-1})$ . The nonhydrogenic spectrum at  $\epsilon \gtrsim 0$  thus oscillates about unity, like the hydrogenic series of modulations  $H_{ii}^F - 1$  and at the same positions, but the modulations are inverted<sup>14</sup> when  $\cos 2\pi \mu_i$  is negative (e.g.,  $\mu_i$

$= 2.65$  in Rb<sup>1</sup>). In the limit  $F \rightarrow 0$ , the modulating factor  $\langle \Psi' | \Psi \rangle^{-1}$  reduces the cross section (12) at  $\epsilon \gtrsim 0$  to its proper continuous and discrete<sup>11</sup> limits and the interference terms with  $l' \neq l$  vanish.

The threshold modulations depend on light polarization through the  $m$  dependence of the polynomial  $U_{\beta i} \propto a_{\beta i}$ . They are largest for minimum  $|m|$  (usually  $m = 0$ ) and maximum  $l - |m|$  in the final state.<sup>3</sup> The extension of Eq. (12) to  $jj$ -coupled final states  $\Psi_j$  is straightforward, though the analogs of Eqs. (13) and (14) are more complicated. The procedures developed here should apply as well to other external fields, to non-alkali atoms, to molecular systems, and even to other processes, as a result of the general nature of the derivation of Eq. (12).

The author is grateful to Professor U. Fano for his many helpful comments regarding this work and the manuscript; to Dr. K. T. Cheng for a calculation of Na oscillator strengths; to Dr.

H. Metcalf and Dr. T. Bergeman for providing the data for the figure; and to Dr. S. Liberman, Laboratoire Aimé Cotton, Orsay, for earlier unpublished Na data that stimulated the present work. This research was supported by the U. S. Department of Energy, Office of Basic Energy Sciences.

<sup>(a)</sup>Present address: National Bureau of Standards, Phy. A-153, Washington, D. C. 20234.

<sup>1</sup>For Rb: R. R. Freeman, N. P. Economou, G. C. Bjorklund, and K. T. Lu, Phys. Rev. Lett. **41**, 1463 (1978); R. R. Freeman and N. P. Economou, Phys. Rev. A **20**, 2356 (1979); see also S. Feneuille, S. Liberman, J. Pinard, and A. Taleb, Phys. Rev. Lett. **42**, 1404 (1979). For Na: W. Sandner, K. A. Safinya, and T. F. Gallagher, Phys. Rev. A **23**, 2448 (1981); S. Liberman, unpublished.

<sup>2</sup>T. S. Luk, L. DiMauro, T. Bergeman, and H. Metcalf, Phys. Rev. Lett. **47**, 83 (1981).

<sup>3</sup>D. A. Harmin, to be published.

<sup>4</sup>D. A. Harmin, Phys. Rev. A **24**, 2491 (1981).

<sup>5</sup>E. Luc-Koenig and A. Bachelier, Phys. Rev. Lett. **43**, 921 (1979), and J. Phys. B **13**, 1743, 1769 (1980).

<sup>6</sup>W. L. Wiese, M. W. Smith, and B. M. Miles, *Atomic Transition Probabilities II*, U. S. National Bureau of

Standards, National Stand. Ref. Data Ser.—22 (U. S. Government Printing Office, Washington, D. C., 1969).

<sup>7</sup>U. Fano, Phys. Rev. A **24**, 619 (1981).

<sup>8</sup>See, e.g., L. D. Landau and E. M. Lifshitz, *Quantum Mechanics (Non-Relativistic Theory)* (Pergamon, Oxford, 1976), 3rd ed., Secs. 36 and 37.

<sup>9</sup>See, e.g., C. H. Greene, U. Fano, and G. Strinati, Phys. Rev. A **19**, 1485 (1979). The applicability of quantum-defect theory to the Stark effect was pointed out by U. Fano, Colloq. Int. CNRS **273**, 130 (1977).

<sup>10</sup>See Ref. 7, Sec. 77. In Ref. 3,  $\Xi(\xi)$  and  $\Upsilon(\eta)$  are called  $\chi_1(\xi)$  and  $\chi_2(\eta)$ .

<sup>11</sup>At  $\epsilon \lesssim 0$ , the wave functions (3) are normalized "per unit energy" by the factor  $(d\nu/d\epsilon)^{1/2} = \nu^{3/2}$ . This implies the usual replacement of the discrete oscillator strengths  $f_n$  by the average density  $df/d\epsilon \equiv \nu^3 f_n$ , which matches smoothly onto  $df/d\epsilon$  at  $\epsilon \gtrsim 0$ . It is this interpolated average which is modulated by  $\langle \Psi' | \Psi \rangle^{-1}$ .

<sup>12</sup>This follows from writing Eq. (10) in terms of the eigenvalues  $\Lambda$  and the eigenvector matrix  $W_{l\Lambda}$  of the product  $[(1 - \hbar^F \tan \delta)^{-1} (H^F \tan \delta)]_{l'l} = \sum_{\Lambda} W_{l'\Lambda} \Lambda (W^{-1})_{\Lambda l}$ , where  $0 \leq l' \leq 2$  or  $3$ .

<sup>13</sup>Equation (13) is exact for a single  $\delta_l \neq 0$  and  $l=l'$ .

<sup>14</sup>This effect would give rise to an *apparent* phase shift of the hydrogenic modulations by  $180^\circ$ . However, since  $H_{l'l}^F$  is asymmetric at  $\epsilon \approx 0$ —the peaks are steeper on the low-energy side—an actual inversion should be observable.